

Training the parametric interactions in an analog bosonic quantum neural network with Fock basis measurement

J. Dudas,¹ B. Carles,¹ E. Gouzien,² J. Grollier,¹ and D. Marković¹

¹Laboratoire Albert Fert, CNRS, Thales, Université Paris-Saclay, 91767 Palaiseau, France

²Alice & Bob, 53 Bd du Général Martial Valin, 75015 Paris, France

(Dated: December 2, 2024)

Quantum neural networks have the potential to be seamlessly integrated with quantum devices for the automatic recognition of quantum states. However, performing complex tasks requires a large number of neurons densely connected through trainable, parameterized weights—a challenging feat when using qubits. To address this, we propose leveraging bosonic modes and performing Fock basis measurements, enabling the extraction of an exponential number of features relative to the number of modes. Unlike qubits, bosons can be coupled through multiple parametric drives, with amplitudes, phases, and frequency detunings serving dual purposes: data encoding and trainable parameters. We demonstrate that these parameters, despite their differing physical dimensions, can be trained cohesively using backpropagation to solve benchmark tasks of increasing complexity. Furthermore, we show that training significantly reduces the number of measurements required for feature extraction compared to untrained quantum neural networks, such as quantum reservoir computing.

The potential of quantum systems for computing has long been recognized, rooted in their ability to exist in superposition and entangled states. These unique properties suggest that quantum computers could outperform classical systems, especially in tasks that leverage parallelism at the quantum level. However, developing algorithms that can effectively encode computational problems into quantum states, exploiting their parallelism, and reliably extracting a single solution has proven to be a significant challenge. As a result, the repertoire of quantum algorithms remains relatively limited [1–3]. Conversely, machine learning has revolutionized problem-solving by optimizing parameterized models to perform specific tasks on input data without the need for explicit algorithmic formulation. This begs the question: could similar techniques be applied to train quantum systems to compute?

One approach to quantum machine learning is through parameterized quantum circuits (PQC), where gate parameters are trained similarly to weights in neural networks. PQC can be trained in a hybrid manner, with the quantum circuit executing the forward pass and a classical computer updating the parameters via gradient descent [4]. This method has yielded promising results, such as in the classification of images [5], quantum phases [6], learning on quantum systems [7], and synthesizing data using a quantum system through generative modeling [8, 9]. However, the scalability of PQCs suffers from the fact that their transfer function is not differentiable, and gradients are calculated through parameter shift rules, by executing the whole circuit twice for each parameter [10].

We propose to implement a quantum neural network (QNN) on a set of parametrically-coupled bosonic Gaussian modes, with neural outputs obtained as Fock state probabilities using Gaussian boson sampling. In this

framework, the weights correspond to the transition rates between different Fock states. Unlike qubits, bosonic modes can be coupled through multiple parametric processes simultaneously, whose amplitudes, phases and frequency detunings we propose to treat as trainable parameters, as well as use for data encoding. A key challenge in this setting arises from the differing physical dimensionalities of these parameters and their simultaneous influence on multiple transition rates. Interestingly, in Gaussian systems, the gradients of Fock state probabilities with respect to these parameters can be expressed analytically. This allows us to implement *physics-aware training* [11], a recently developed method for classical neuromorphic computing that leverages the physical system for the forward pass while performing backpropagation in a model.

We consider a set of M driven bosonic modes, pairwise coupled through two parametric processes: coherent photon conversion at a rate g_{kl} and two-mode squeezing at a rate g^s_{kl} for modes k and l (Figure 1a). This type of interaction can be obtained in circuit Quantum Electrodynamics (cQED) using tunable parametric couplers [12]. In the rotating frame, the Hamiltonian of this system writes:

$$\begin{cases} \hat{H} = \hat{H}_0 + \hat{H}_{\text{in}} \\ \hat{H}_0 = - \sum_{k=1}^M \delta_k \hat{a}_k^\dagger \hat{a}_k + \sum_{k<l} g_{kl} \hat{a}_k^\dagger \hat{a}_l + g^s_{kl} \hat{a}_k^\dagger \hat{a}_l^\dagger + \text{h.c.} \\ \hat{H}_{\text{in}} = i\hbar \sum_k \sqrt{\kappa_k} \hat{a}_k \hat{a}_{k,\text{in}}^\dagger + \text{h.c.} \end{cases}, \quad (1)$$

where \hat{H}_0 and \hat{H}_{in} are respectively the Hamiltonians describing the evolutions of the M coupled bosonic modes and their interactions with the input drives, δ_k is the drive detuning of the mode k from its resonance frequency and κ_k is its coupling to the transmission line. The input modes $\hat{a}_{k,\text{in}}$ are in coherent states of ampli-

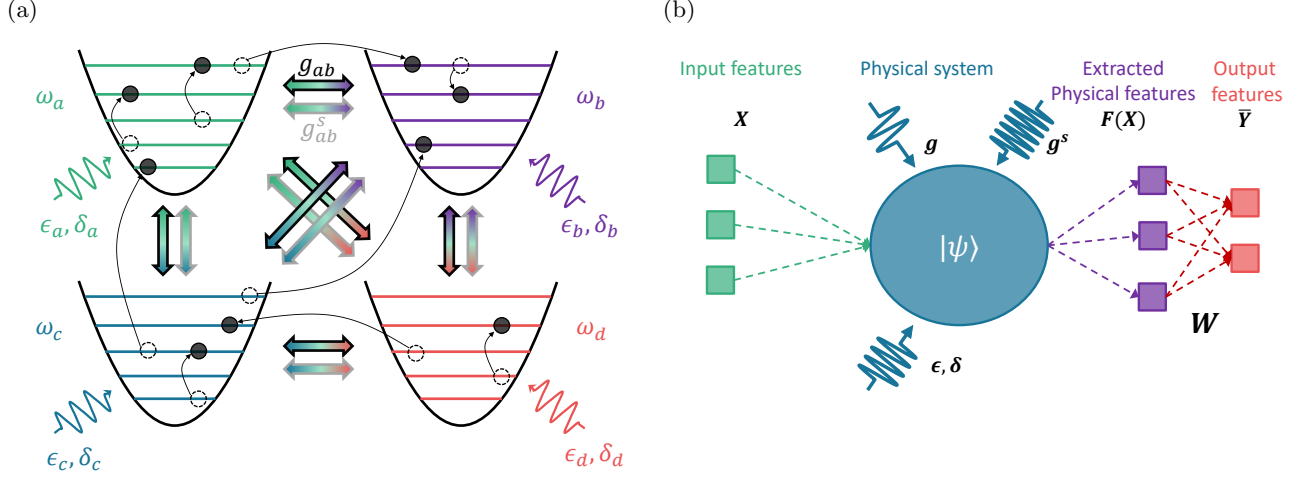


FIG. 1: (a) A set of bosonic modes (here 4), driven close to resonance at frequencies $\omega_k + \delta_k$, at amplitudes ϵ_k with dissipation rates κ_k . Two types of coupling processes are driven, photon exchange at a rate g_{kl} (dark gray arrow) and two-mode squeezing at a rate g_{kl}^s (light gray arrow). (b) Schematic of an analog quantum neural network. Input data vector \mathbf{X} (green squares) is encoded into drive parameters, and feature vector $\mathbf{F}(\mathbf{X})$ (purple squares) is obtained by measuring probabilities $P_k(n)$ of a mode k to contain n photons. Prediction $\bar{\mathbf{Y}}$ (red squares) is obtained by multiplying the feature vector by a trained weight matrix \mathbf{W} .

tude $\epsilon_k = \langle \hat{a}_{k,\text{in}} \rangle$; the system is in a Gaussian state [13] and thus fully described by its displacement vector $\boldsymbol{\alpha}$ and covariance matrix $\boldsymbol{\sigma}$, and its dynamics are linear. In order to implement a quantum neural network capable of transforming nonlinearly separable input data into linearly separable features, we need to introduce a nonlinear operation into our system. We achieve this by performing photon number resolving measurements, in the Fock basis, and deducing the probabilities $P_k(n)$ of the mode k to contain n photons from the statistics of the measurement outcomes. An analog bosonic quantum neural network is thus obtained by encoding the input data into the system's drive parameters, and after some time evolution, measuring occupation probabilities that are nonlinear functions of these inputs (Figure 1b).

We train two layers of weights, the complex drive parameters, that is, the amplitudes, phases, and detunings of the nearly resonant drives, as well as the amplitudes and phases of the coupling tones, and the output weights \mathbf{W} . Detunings of the coupling tones are not free parameters, as in the rotating wave approximation, they are only efficient if they are set to $\delta_{kl}^s = \frac{1}{2}(\delta_k + \delta_l)$ for the two-mode squeezing tone and $\delta_{kl} = \frac{1}{2}(\delta_k - \delta_l)$ for the coherent photon conversion tone. All physical parameters can be represented in vectors: $\boldsymbol{\epsilon}$ stores the drives, $\boldsymbol{\delta}$ the detunings, \mathbf{g} the photon conversion rates, \mathbf{g}^s the two-mode squeezing rates and $\boldsymbol{\kappa}$ the transmission line couplings. Depending on the task, we choose to encode the input data \mathbf{x} in one of these variables

$$\boldsymbol{\theta} = \boldsymbol{\theta}_0^T \mathbf{x} + \boldsymbol{\theta}_{\text{bias}}, \quad (2)$$

while the others, as well as the prefactor $\boldsymbol{\theta}_0$, bias $\boldsymbol{\theta}_{\text{bias}}$

of the encoding variable and \mathbf{W} , are treated as trainable parameters. The Fock state occupation probabilities are given by Gaussian boson sampling (GBS) [14]

$$P_k(n|\boldsymbol{\alpha}, \boldsymbol{\sigma}) = \frac{\exp(-\frac{1}{2}\boldsymbol{\alpha}_k^\dagger \boldsymbol{\sigma}_{k,Q}^{-1} \boldsymbol{\alpha}_k)}{n! \sqrt{\det(\boldsymbol{\sigma}_{k,Q})}} \text{lhaf}(\mathbf{A}_n), \quad (3)$$

where

$$\begin{cases} \boldsymbol{\sigma}_{k,Q} &= \boldsymbol{\sigma}_k + \mathbb{1}_2/2 \\ \mathbf{T} &= \begin{pmatrix} 0 & 1 \\ 1 & 0 \end{pmatrix} \\ \mathbf{A} &= \mathbf{T} \left(\mathbb{1}_2 - \boldsymbol{\sigma}_{k,Q}^{-1} \right) \end{cases}, \quad (4)$$

$\boldsymbol{\alpha}_k$ and $\boldsymbol{\sigma}_k$ are the displacement vector and the covariance matrix of the mode k , and $\mathbb{1}_2$ and $\mathbb{0}_2$ are respectively the unitary and zero matrices in two dimensions. \mathbf{A}_n is formed from \mathbf{A} by substituting its diagonal with $\boldsymbol{\alpha}_k^\dagger \boldsymbol{\sigma}_{k,Q}^{-1} \boldsymbol{\alpha}_k$, then repeating the 1st and 2nd rows and columns n times and $\text{lhaf}(\cdot)$ is the loop hafnian function [15]. Analytical gradients are obtained through automatic differentiation and the parameters are optimized with the Adam Optimization algorithm [16] in PyTorch, based on a code adapted from [17].

We first benchmark this bosonic neural network on the sine and square waveform classification task (Figure 2). For this task, we use two bosonic modes and encode the input data x into their nearly resonant drive amplitudes ϵ_k . The input data points are sent one by one, each for a duration of $\delta t = 100$ ns. The drive amplitudes are limited to a range that ensures negligible probability amplitudes for photon states higher than 9. The loss function applied for this task is the mean square error (MSE),

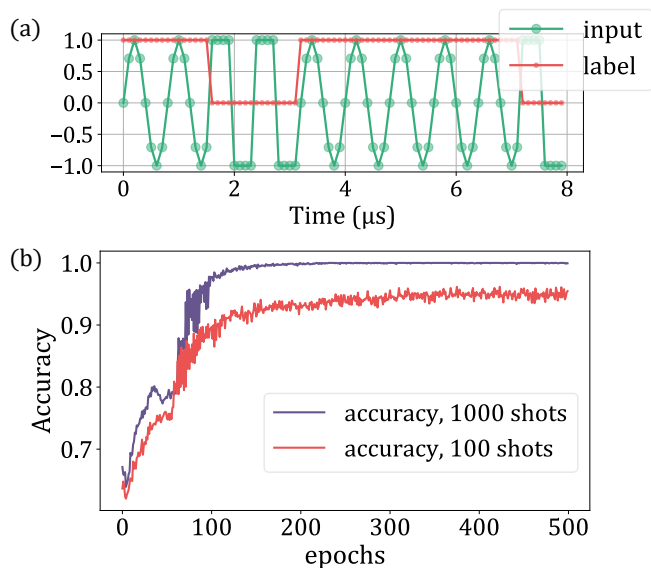


FIG. 2: Sine/square classification task. (a) The input data is a time series of points belonging to a random series of sine or square waveforms, each discretized into 8 points. The task consists in predicting to which waveform the point belongs. (b) Accuracy as a function of the number of training epochs for two different numbers of measurement shots used to determine probability $P_1(0)$.

$f(\bar{\mathbf{Y}}, \mathbf{Y}) = (1/N) \sum_{i=1}^N (\bar{\mathbf{Y}}_i - \mathbf{Y}_i)^2$, where N is the number of data points used for training, $\bar{\mathbf{Y}} = \mathbf{W}\mathbf{F}(\mathbf{X})$ is the network prediction obtained by multiplying the feature vector $\mathbf{F}(\mathbf{X})$ containing the measured probabilities by the weights matrix \mathbf{W} , and \mathbf{Y} is the target. Parameter values are constrained within a physically achievable range for superconducting circuits. To prevent the training from pushing the parameters to values that cause photon numbers to diverge, we introduce a regularization to the loss function, $\text{loss}_{\langle \bar{N} \rangle} = \beta_{\langle \bar{N} \rangle} \times \text{MSE}(\langle \bar{N} \rangle_{\text{avg}}, \langle \bar{N} \rangle_{\text{tg}})$, where $\langle \bar{N} \rangle_{\text{avg}}$ is a vector containing the average photon number expectation values $\langle \bar{N} \rangle$ over the time interval δt , obtained by allowing the system dynamics to evolve with a maximal value input and the target average photon number $\langle \bar{N} \rangle_{\text{tg}}$ is set to 2 photons in each mode. The parameter $\beta_{\langle \bar{N} \rangle}$ is a prefactor that controls the influence of $\text{loss}_{\langle \bar{N} \rangle}$ on the overall learning process. The total optimized loss is then $f(\bar{\mathbf{Y}}, \mathbf{Y}) + \text{loss}_{\langle \bar{N} \rangle}$. The results are summarized in Table 1. We compare the performance of the bosonic QNN to quantum reservoir computing with coupled bosonic modes [18]. In the quantum reservoir, the parameters within the quantum system are not trained, and only the output weights that multiply the measured output neurons are learned. Training the drive parameters reduces the number of required observables to measure down to just one, i.e. the probability of having 0 photons in the first mode $P_1(0)$, compared to 9 for

	N_{out}	N_{shots}
Quantum reservoir [18]	9	10^8
Bosonic QNN	1	10^3

TABLE I: Number of observables and measurement shots required to reach 100 % accuracy on the sine-square classification task for quantum reservoir and for bosonic QNN.

quantum reservoir. This provides a twofold reduction in the number of measurements to perform: (1) the total number of observables to measure is reduced, and (2) as $P_k(0) > P_k(n > 0)$, fewer measurement shots are needed to accurately determine the probability [19]. The bosonic QNN achieves 100 % accuracy with 10^3 measurement shots (Figure 2(b)), in contrast to the 10^8 measurement shots required for the quantum reservoir [17].

Another advantage of analog quantum neural networks is that the choice of the encoding parameter influences the nonlinear transformation that the quantum system applies to the input data. To investigate the question of the optimal encoding parameter, we use the spiral classification task (Figure 3(a)), which has two-dimensional inputs, and is known to require more nonlinearity than the sine-square classification. We use four coupled modes and compare the encoding into six different variables: the amplitude and phase of the nearly resonant drives, the exchange coupling tone, and the two-mode squeezing tone (Figure 3(a)). We use the Binary Cross Entropy (BCE) with logits loss (see Supp. Mat.) for this task. We find that encoding into either the amplitude or phase of the two-mode squeezing achieves 100 % performance with just a single measured probability. In contrast, encoding into the drive phase requires 12 measured probabilities to reach 96 % accuracy, while the other methods plateau at 80–90 % accuracy. This can be understood by noticing that two-mode squeezing has a more significant impact on the covariance matrix than the coherent photon exchange (see section ?? of Supp. Mat.). In particular, if there is no two mode squeezing, the covariance matrix $\sigma(t)$ does not evolve beyond its initial vacuum value $\sigma_0 = 1/2$, independently of the values $\{\delta, \epsilon, \mathbf{g}\}$.

Parametrized quantum circuits often face convergence challenges due to vanishing gradients in flat function landscapes—a phenomenon known as barren plateaus [20–22], and commonly attributed to excessive entanglement in qubit systems. Notably, it has been shown that cost functions utilizing local observables, as opposed to global ones, are less susceptible to barren plateaus [22, 23]. The occurrence of barren plateaus in bosonic systems, however, remains an open question and is not yet fully understood [24]. In our work, we have trained the bosonic QNN on the spirals classification task for 6, 8, or 10 modes. We have compared a local cost

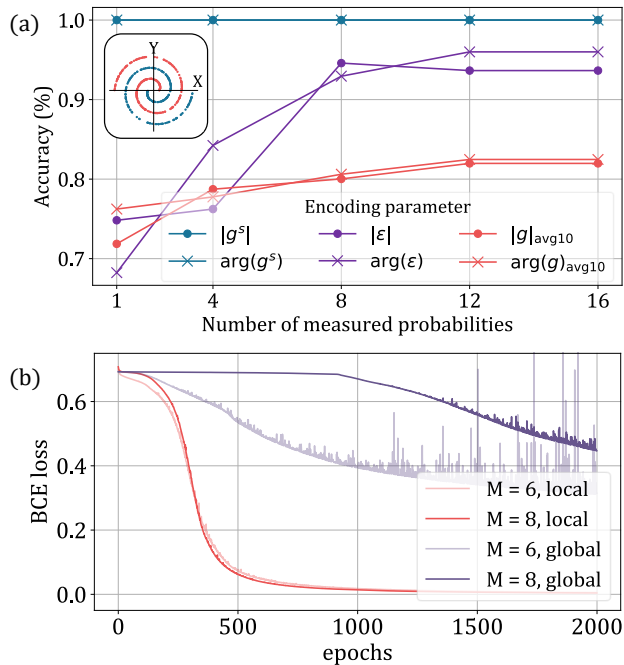


FIG. 3: (a) Spiral classification task consists in assigning a point to the blue or red spiral (inset). The non-linearity of the task is apparent in that it is impossible to draw a straight line to separate the two spirals. The accuracy for different encoding schemes is shown as a function of the number of measured probabilities. Since the accuracies obtained when encoding in \mathbf{g} or $\arg(\mathbf{g})$ vary greatly with the initial physical parameters $\{\mathbf{g}; \mathbf{g}^s; \delta; \epsilon\}$, we average the accuracies obtained with this encoding over 10 initial sets of parameters. (b) Minimization of the BCE with logits loss for number of modes $M \in \{6, 8\}$ with either local (red) or global (purple) cost function.

function involving $P_1(0)$ with a global cost function that incorporates the joint probability to have 0 photons in each of the M modes (Figure 3(b)). Our observations show that learning with local cost functions is considerably faster than with global ones.

In order to pin down the advantage brought by the training of the quantum system parameters, as well as the advantage brought by the quantum nature of the neural network, we compare the resources in terms of the number of parameters that need to be trained, and the number of outputs that need to be measured in order to reach 100% accuracy on the spirals task for a classical Liquid Echo State Network (LESN) [25], a Multi-Layer Perceptron (MLP), quantum reservoir and bosonic QNN. The results are summarized in Table II. We observe that bosonic QNN needs a smaller number of trainable parameters compared to classical neural networks and a significantly smaller number of observables to measure compared to quantum reservoir computing.

	LESN	MLP	Quantum reservoir	Bosonic QNN
layers	2	2	1	1
outputs	64	5	36	1
parameters	64	61	37	38

TABLE II: Number of neurons and parameters needed to reach 100% accuracy on the spiral classification task using LESN, MLP, quantum reservoir and bosonic QNN.

	SLP	MLP	Spintronic NN	Bosonic QNN
layers	1	2	3	1
layer size	10	8	32	12
parameters	578	559	2992	442

TABLE III: Number of neurons and parameters needed to reach 97% accuracy on the DIGITS task using a classical Single Layer Perceptron, Multi-Layer Perceptron, and bosonic QNN. The classical spintronic neural network reaches 89.83% accuracy.

A bosonic neural network that we propose has the advantage of a large Hilbert space for feature encoding, that scales exponentially with the number of modes, but faces a challenge of a limited number of parameters available for encoding and training, that is linear in the number of modes. By consequence, highly dimensional data, such as images, cannot be processed in a single time step. We address this issue by employing an encoding scheme inspired by the data reuploading method [26] and demonstrate it on the DIGITS dataset (Figure 4(a)), consisting of 8×8 pixel images of handwritten digits. We use 6 modes, pairwise coupled through 15 two-mode squeezing and 15 coherent drives. The whole 64 pixel image cannot be encoded in a single time step – we thus divide each input image into batches of 15 pixels, that we encode into the phases of 15 two-mode squeezing drives applied over 4 time intervals $\delta t/4 = 50 \text{ ns} \ll \kappa^{-1} = 500 \text{ ns}$ (Figure 4(b)). Using this method, we achieve over 97% accuracy on the DIGITS classification task, by measuring 12 probability amplitudes $P_k(n)$ and a training a total of 442 drive parameters and output weights. As shown in Table III, the number of parameters required for training in the bosonic neural network is reduced by 20% compared to classical neural networks (SLP and MLP) and is 6 times smaller compared to a classical dynamical hardware neural network, which achieves an accuracy of 89.83% [27].

In this work, we have shown that an analog bosonic quantum neural network can be trained using physics aware training and backpropagation applied to the complex parameters of the three-wave mixing parametric interactions and nearly resonant drives. By training the quantum system, we have reduced the number of vari-

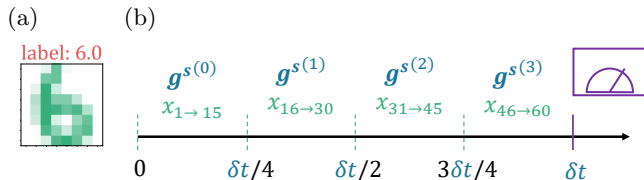


FIG. 4: (a) A sample from the DIGITS dataset, consisting of an 8×8 image and its corresponding label. To create a flattened image vector of size 60, we crop the corners of the original image. The dataset contains 1500 samples, each belonging to one of 10 classes. (b) The encoding scheme utilizes 6 modes. At times 0, $\delta t/4$, $\delta t/2$, and $3\delta t/4$, 15 pixels are encoded into 15 two-mode squeezing drives, denoted by g_{kl}^s . During each data re-uploading instance, a new set of parameters $\{g, g^s, \delta, \epsilon\}$ is applied. At time δt , the Fock state probabilities are measured, yielding the feature vector $F(\mathbf{X})$.

ables to measure for feature extraction. For both the sine/square classification and spirals classification tasks, the number of variables to measure has been reduced to a single one, compared to 9 and 36, respectively, in untrained quantum reservoir computing. Using 6 bosonic modes and data reuploading, we have demonstrated classification of 64-dimensional images from the DIGITS dataset, with 442 trained parameters, compared to 578 parameters for the classical single layer perceptron.

Compared to the parametrized quantum circuits, that are trained using parameter-shift method, physics aware training reduces the number of measurements by a factor of 2 for each trained parameter. Instead of discrete gates used in PQCs, we apply continuous interactions at different frequencies to drive different processes. This reduces the hardware complexity, and allows to model the transfer function of the quantum neural network, and by consequence to obtain an analytic expression for the gradients. Compared to the implementations with qubits, the use of bosonic modes reduces the number of physical devices to couple to achieve the same size of the Hilbert space for the feature embedding. Further research is needed to deepen our understanding of the scalability of bosonic neural networks, and their robustness to decoherence and the emergence of barren plateaus when they are scaled up.

ACKNOWLEDGMENTS

This research was supported by the European Union (ERC, qDynnet, 101076898). Views and opinions expressed are however those of the author(s) only and do not necessarily reflect those of the European Union or

the European Research Council. Neither the European Union nor the granting authority can be held responsible for them.

AUTHOR CONTRIBUTIONS

D.M. and J.G. conceived the project. J.D. and E.G. performed the calculations, J.D. performed the quantum simulations. B.C. participated to analytical calculations and quantum simulations. D.M. and J.D. wrote the manuscript.

COMPETING INTERESTS

The authors declare no competing interests.

-
- [1] L. K. Grover, in *Proceedings of the Twenty-Eighth Annual ACM Symposium on Theory of Computing*, STOC '96 (Association for Computing Machinery, New York, NY, USA, 1996) pp. 212–219.
 - [2] P. W. Shor, *SIAM J. Comput.* **26**, 1484 (1997).
 - [3] A. W. Harrow, A. Hassidim, and S. Lloyd, *Phys. Rev. Lett.* **103**, 150502 (2009).
 - [4] M. Benedetti, E. Lloyd, S. Sack, and M. Fiorentini, *Quantum Sci. Technol.* **4**, 043001 (2019).
 - [5] X. Ding, Z. Song, J. Xu, Y. Hou, T. Yang, and Z. Shan, *Sci Rep* **14**, 15886 (2024).
 - [6] J. Herrmann, S. M. Llima, A. Remm, P. Zapletal, N. A. McMahon, C. Scarato, F. Swiadek, C. K. Andersen, C. Hellings, S. Krinner, N. Lacroix, S. Lazar, M. Kerschbaum, D. C. Zanuz, G. J. Norris, M. J. Hartmann, A. Wallraff, and C. Eichler, *Nat Commun* **13**, 4144 (2022).
 - [7] H.-Y. Huang, M. Broughton, J. Cotler, S. Chen, J. Li, M. Mohseni, H. Neven, R. Babbush, R. Kueng, J. Preskill, and J. R. McClean, *Science* **376**, 1182 (2022).
 - [8] M. Benedetti, D. Garcia-Pintos, O. Perdomo, V. Leyton-Ortega, Y. Nam, and A. Perdomo-Ortiz, *npj Quantum Inf* **5**, 1 (2019).
 - [9] L. Hu, S.-H. Wu, W. Cai, Y. Ma, X. Mu, Y. Xu, H. Wang, Y. Song, D.-L. Deng, C.-L. Zou, and L. Sun, *Science Advances* **5**, eaav2761 (2019).
 - [10] M. Schuld, V. Bergholm, C. Gogolin, J. Izaac, and N. Killoran, *Phys. Rev. A* **99**, 032331 (2019).
 - [11] L. G. Wright, T. Onodera, M. M. Stein, T. Wang, D. T. Schachter, Z. Hu, and P. L. McMahon, *Nature* **601**, 549 (2022).
 - [12] A. Metelmann, *SciPost Physics Lecture Notes*, 066 (2023).
 - [13] G. Adesso, S. Ragy, and A. R. Lee, *Open Syst. Inf. Dyn.* **21**, 1440001 (2014).
 - [14] C. S. Hamilton, R. Kruse, L. Sansoni, S. Barkhofen, C. Silberhorn, and I. Jex, *Phys. Rev. Lett.* **119**, 170501 (2017).

- [15] A. Björklund, B. Gupt, and N. Quesada, A faster hafnian formula for complex matrices and its benchmarking on a supercomputer (2019), arXiv:1805.12498 [quant-ph].
- [16] D. P. Kingma and J. Ba, Adam: A Method for Stochastic Optimization (2017), arXiv:1412.6980 [cs].
- [17] J. F. F. Bulmer, B. A. Bell, R. S. Chadwick, A. E. Jones, D. Moise, A. Rigazzi, J. Thorbecke, U.-U. Haus, T. Van Vaerenbergh, R. B. Patel, I. A. Walmsley, and A. Laing, Science Advances **8**, eabl9236 (2022).
- [18] J. Dudas, B. Carles, E. Plouet, F. A. Mizrahi, J. Grollier, and D. Marković, npj Quantum Inf **9**, 1 (2023).
- [19] S. A. Khan, F. Hu, G. Angelatos, and H. E. Türeci, Physical reservoir computing using finitely-sampled quantum systems (2021), arXiv:2110.13849 [quant-ph].
- [20] S. Wang, E. Fontana, M. Cerezo, K. Sharma, A. Sone, L. Cincio, and P. J. Coles, Nat Commun **12**, 6961 (2021).
- [21] Z. Holmes, K. Sharma, M. Cerezo, and P. J. Coles, PRX Quantum **3**, 010313 (2022).
- [22] A. V. Uvarov and J. D. Biamonte, J. Phys. A: Math. Theor. **54**, 245301 (2021).
- [23] M. Cerezo, A. Sone, T. Volkoff, L. Cincio, and P. J. Coles, Nat Commun **12**, 1791 (2021).
- [24] R. A. Bravo, J. G. Ponce, H.-y. Hu, and S. F. Yelin, Circumventing Traps in Analog Quantum Machine Learning Algorithms Through Co-Design (2024), arXiv:2408.14697 [quant-ph].
- [25] A. Senanian, S. Prabhu, V. Kremenetski, S. Roy, Y. Cao, J. Kline, T. Onodera, L. G. Wright, X. Wu, V. Fatemi, and P. L. McMahon, Nat Commun **15**, 7490 (2024).
- [26] A. Pérez-Salinas, A. Cervera-Lierta, E. Gil-Fuster, and J. I. Latorre, Quantum **4**, 226 (2020).
- [27] E. Plouet, D. Sanz-Hernández, A. Vecchiola, J. Grollier, and F. Mizrahi, Training a multilayer dynamical spintronic network with standard machine learning tools to perform time series classification (2024), arXiv:2408.02835 [cond-mat].